Dalton Transactions

Cite this: *Dalton Trans.*, 2012, **41**, 12349

www.rsc.org/dalton

COMMUNICATION

Ytterbium can relax slowly too: a field-induced Yb_2 single-molecule magnet†

Po-Heng Lin,[a] Wen-Bin Sun,*[b] Yong-Mei Tian,[b] Peng-Fei Yan,*[b] Liviu Ungur,[c] Liviu F. Chibotaru*[c] and Muralee Murugesu*[a]

Received 25th July 2012, Accepted 15th August 2012
DOI: 10.1039/c2dt31677c

An unusual dinuclear Yb_2 complex isolated using a mixed ligand strategy leads to field-induced SMM behaviour. Low magnetic axiality and a large tunnelling gap lead to significant quantum tunnelling of the magnetisation, which was reduced under an applied static optimum field of 1600 Oe.

Since the discovery of lanthanide single-molecule magnets (SMMs) in 2003,[1] researchers have actively been searching for new lanthanide based SMMs. This is mainly due to the fact that lanthanide SMMs clearly surpassed energy barriers displayed by transition metal systems.[2] In lanthanide systems, a large intrinsic magnetic anisotropy contribution leads to magnet-like behaviour of slow relaxation of the magnetisation at low temperatures. Thus, recent research has led to the discovery of molecular complexes with Tb^{III},[3] Dy^{III},[3c,4] Ho^{III},[5] Er^{III},[6] Tm^{III},[7a] and Yb^{III},[7] to behave as SMMs. Among these ions Dy^{III} has so far been the most prolific in this quest. However, larger energy barriers must be achieved to move towards application of these materials in technologies such as memory storage. Towards this goal other systems need to be investigated; new ligand design and new metal ions are obvious strategies to pursue.

Recently, Long and co-workers predicted that Yb^{III} ions could also lead to SMM behaviour if an appropriate ligand system is employed.[2c] Although the Yb^{III} ion is highly anisotropic, only two single-ion magnets have been reported so far.[7] No larger polynuclear complexes have been reported to date. In order to create polynuclear Yb based SMMs we need to develop a specific synthetic strategy where magnetic anisotropy of the Yb^{III} ion will be enhanced through an appropriate ligand system.

As a proof of concept we have synthesised the Yb^{III} analogue of our recently reported Dy^{III} complex and studied its magnetic properties.[8] The reported complex exhibits slow relaxation of the magnetisation under an applied dc field. To our knowledge this field-induced SMM behaviour for a polynuclear Yb^{III} complex has never been reported.

Our synthetic approach relies on the employment of a mixed ligand strategy where the presence of salen type ligand L (Scheme S1, ESI†) is ideal for coordination of metal ions as well as promoting magnetic interaction through phenoxide bridges. The use of $Yb(acac)_3$ as the synthetic precursor leads to coordination of $acac^-$ ligands to complete the coordination sphere of the lanthanide ions. We have recently reported the synthesis of a $[Dy_2L_2(acac)_2(H_2O)]$ analogue, thus by following the same synthetic procedure $[Yb_2L_2(acac)_2(H_2O)]\cdot 2CH_2Cl_2$, **1**, was isolated.[8]

Complex **1** crystallises in the monoclinic $P2_1/n$ space group where the molecular structure is shown in Fig. 1 and S1.† The structure is composed of two Yb^{III} ions located slightly out of the N_2O_2 coordination pocket of two L^{2-} ligands as the Yb^{III} ions are larger than transition metal ions. Two $acac^-$ ligands and one H_2O molecule complete the coordination environment of the lanthanide ions. The Yb1 atom is in an octacoordinate distorted square antiprism geometry whereas Yb2 displays a heptacoordinate distorted capped trigonal prism. The intramolecular Yb1···Yb2 distance of 3.79 Å and the average Yb–O–Yb angle

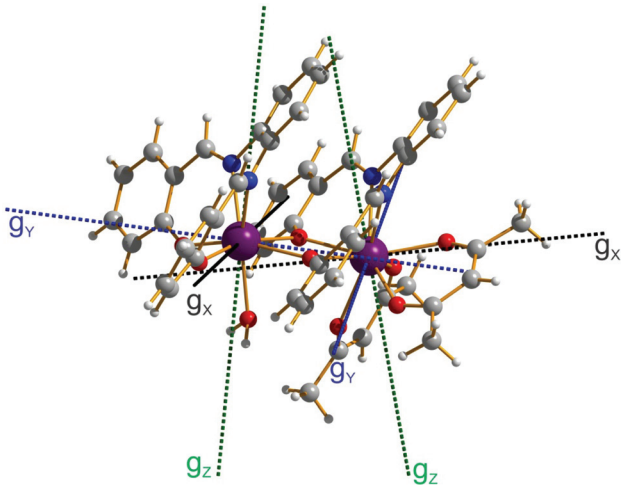

Fig. 1 Molecular structure of $[Yb_2L_2(acac)_2(H_2O)]$, **1**. Yb1 (right) is in a distorted square antiprism environment, Yb2 (left) is in a distorted capped trigonal prism environment. Colour code: Yb (purple), O (red), N (blue), C (grey), H (white). Orientation of the main anisotropy axes in the ground Kramers doublet is given in dashed lines.

[a]*Department of Chemistry, University of Ottawa, 10 Marie-Curie, Ottawa, ON, Canada, K1N 6N5. E-mail: m.murugesu@uottawa.ca*
[b]*Key Laboratory of Functional Inorganic Material Chemistry, Ministry of Education, No. 74, Xuefu Road, Nangang District, Harbin 150080, P.R. China. E-mail: wenbinsun@yahoo.cn*
[c]*Division of Quantum and Physical Chemistry and INPAC—Institute for Nanoscale Physics and Chemistry, Katholieke Universiteit Leuven, Celestijnenlaan, 200F, 3001 Leuven, Belgium*

†Electronic supplementary information (ESI) available: Additional structural, magnetic computational data can be found there. CCDC 830606. For ESI and crystallographic data in CIF or other electronic format see DOI: 10.1039/c2dt31677c

of 111.2° are similar to those of the recently reported isostructural Dy_2 complex.[8] Additionally, complex **1** also reveals 5.94 Å as the closest intermolecular Yb2···Yb2 distance (Fig. S2†). Moreover, the hydrogen atom H9 bonded to the O9 atom hydrogen bonds to the phenoxide oxygen (O3) from the neighbouring molecule forming pairs of hydrogen bonded dinuclear units. It is noteworthy that the O9 atom is 2.33 Å away from its coordinated Yb2 ion and 4.12 Å away from the Yb2 from the neighbouring molecule (Fig. S3†).

The Near Infrared (NIR) fluorescence properties of **1** in the solid state and in CH_2Cl_2, CH_3CN and CH_3OH solutions were studied. Under the above conditions, the typical emission bands of Yb^{III} assigned to the $^2F_{5/2} \rightarrow {}^2F_{7/2}$ transitions are all observed at 975 nm upon excitation at 390 nm. A slightly strong emission was observed in a CH_2Cl_2 solution (Fig. S4†). It is noteworthy that the solvent quenching effect of strong coordination of CH_3OH was not very obvious thanks to the strongly coordinating ability of β-diketonates. The free ligand H_2L does not exhibit NIR fluorescence under similar conditions. These observations are consistent with the NIR fluorescence of **1** in solution arising from the Yb^{III} centre. Besides, the emission spectrum of Yb^{III} ions in **1** reveals not only one sharp main component at 975 nm corresponding to the zero-phonon transition but also broader components at longer wavelengths (lower energy) at 1005 and 1028 nm, which were assigned to the inter-Stark $^2F_{5/2} \rightarrow {}^2F_{7/2}$ transitions.[9]

For **1**, its luminescent decay curves obtained from time-resolved luminescent experiments can be fitted with two exponentials, which is due to the different coordination geometries of the two Yb^{III} ions (Fig. S5†).[9] The decay times (μs) and amplitudes (%) were 2.47 μs (57.29%) and 10.38 μs (42.71%) and the intrinsic quantum yields (0.12% and 0.52%, respectively) of Yb^{III} emission may be estimated by $\Phi_{Ln} = \tau_{obs}/\tau_0$, where τ_{obs} is the observed emission lifetime and τ_0 is the 'neutral lifetime', *i.e.* 2.0 ms for the Yb^{III} ions.[10] The value of the fluorescence lifetimes for **1** is comparable to those of dinuclear ZnLn Schiff base complexes and among the few examples of homo-nuclear lanthanide complexes with Schiff base ligands,[10] which likely results from the quantity of accepting levels of the Yb^{III} ion from the ligands.

Direct current (dc) susceptibility measurement of **1** (Fig. 2) indicates that the χT value of 5.47 cm^3 K mol^{-1} at 300 K is close to the theoretical value of 5.14 cm^3 K mol^{-1} for two non-interacting Yb^{III} ions ($^2F_{7/2}$, J = 7/2, g = 8/7, $\chi T_{free\ ion}$ = 2.57 cm^3 K mol^{-1}). Upon decrease of the temperature, the χT product decreases steadily reaching a minimum value of 3.12 cm^3 K mol^{-1} at 5 K followed by a slight increase at low temperature to reach 3.20 cm^3 K mol^{-1} at 2 K. The initial decrease of the χT product is most likely due to depopulation of the Stark sublevels and/or significant magnetic anisotropy present in Yb^{III} systems. The final increase below 5 K indicates the presence of ferromagnetic interactions between the metal ions as previously seen for the Dy^{III} analogue. Magnetisation measurements (Fig. 2 inset) at low fields indicate a linear increase of the magnetisation while at higher fields the curves increase slightly without complete saturation. Moreover, iso-temperature lines are observed to be close together without completely superimposing. This suggests the presence of a small amount of magnetic anisotropy in the system.

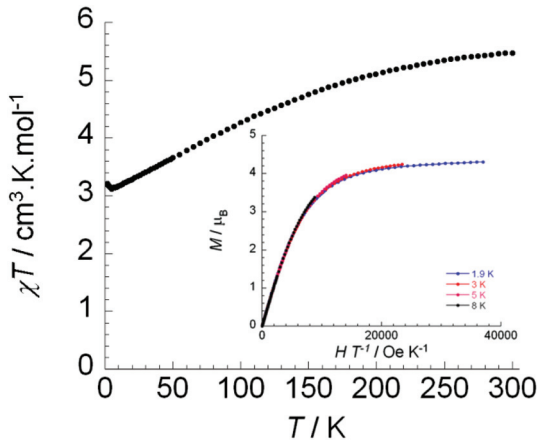

Fig. 2 Temperature dependence of the χT product at 1000 Oe for complex **1** (with χ being the molar susceptibility per dinuclear complex defined as M/H). Inset: M *vs.* H data at various temperatures (1.9, 3, 5 and 8 K) are shown on a single M *vs.* H/T plot.

Ac susceptibility measurements were performed as a function of frequency at variable temperatures to probe any magnet-like behaviour for **1**. In the absence of an applied static field no ac signal was observed; however when a static dc field was applied a clear frequency dependent signal was observed. Such slow relaxation of the magnetisation occurring under an applied dc field generally suggests the presence of significant quantum tunnelling, which reduces the energy barrier. Therefore, to optimize the reduction of the quantum tunnelling it is essential to carry out optimum field scan study (Fig. S6†). The resulting optimum field of 1600 Oe was applied while ac susceptibility measurements were carried out in function of frequency. Under this field a frequency dependent signal was observed below 8 K indicative of field-induced SMM behaviour (Fig. 3). The obtained ac data can be fitted using an Arrhenius equation, which leads to an effective energy barrier of 24.5 K and a $\tau_0 = 6.8 \times 10^{-7}$ s (Fig. S7†).

Such strong field dependence of the relaxation time was recently reported for a $[Yb(dipic)_3]^{3-}$ complex with trigonal D_3 symmetry.[7c] An interesting fact in that report is among all analogous Ln^{III} complexes the Yb has the largest energy barrier (187 K).

In an attempt to perform magneto-structural correlation, a careful inspection of the structure was made. As aforementioned, Yb1 adopts a distorted square antiprism geometry with the metal ion sandwiched in between the O1O2N1N2 and O5O6O7O8 planes whereas Yb2 adopts a rare capped trigonal prism geometry (Fig. S1†). The square plane of the latter prism is formed by O1, O2, O3, O4 atoms with Yb–O distances in the 2.14–2.29 Å range. The clearly longer apical Yb–O; Yb–N distances are in the 2.33–2.44 Å range. Recently, Long and co-workers postulated that contrary to the Dy^{III} ion, the Yb^{III} ion is predicted to have a prolate electron density. Their hypothesis suggests that stronger equatorial coordination is expected to favour the well-separated $m_J = \pm 7/2$ ground state, whereas axial chelation within a square antiprismatic coordination environment should lead to the $m_J = \pm 5/2$ ground state. Significant separation between the ground state and the first excited state is a requisite for strong

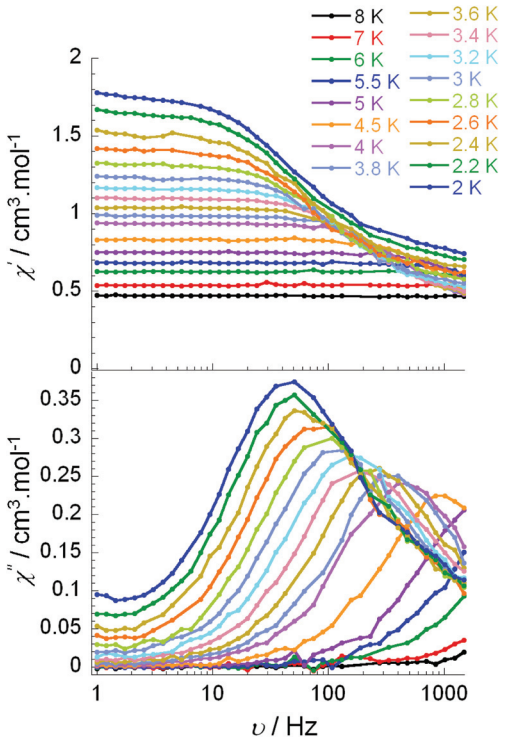

Fig. 3 Frequency dependence of the in-phase χ' (top) and out-of-phase χ'' (bottom) ac susceptibility signals under a 1600 Oe optimum dc-field.

SMM behaviour. Thus from our structural observation and based on the recently postulated hypothesis, it is tempting to conclude that the Yb2 ion might contribute much more than the Yb1 to the magnetic anisotropy.[2c] However this needs to be carefully verified as our system is highly unsymmetrical and two reported examples[7] are counterintuitive. In the reported polyoxometallate–Yb complex,[7a] the Yb^{III} ion adopts a square antiprismatic coordination environment with an $m_J = \pm 5/2$ ground state with the first $m_J = \pm 7/2$ excited state lying only at 100 cm^{-1} above, whereas in the case of the Zn_3Yb complex, an $m_J = \pm 7/2$ ground state was reported with a predominantly equatorial coordination environment thanks to the employment of a macrocyclic ligand.[7b] The former displayed a frequency dependent signal under a zero applied dc field whereas for the latter a dc field of 500 Oe was required to reduce the occurring quantum tunnelling. This gives an indication that the anisotropy might lie in the easy plane in our molecule.

Contrary to that, the two Yb^{III} ions of **1** are in low symmetry environments, far from a square antiprismatic coordination. The *ab initio* calculations of the CASSCF level have been done with the MOLCAS 7.6 package[11a] and the magnetic properties have been calculated with Single_Aniso[11b] and Poly_Aniso modules (see the ESI for the details, Table S1, Fig. S8†). The results show that all four Kramers doublets (KD) corresponding to the atomic multiplet $J = 7/2$ are of easy axis type but are far from being axial (*i.e.*, from being characterized by definite m_J), which is seen from their large transversal g factors (Table S2†). The main magnetic axes on Yb sites are not parallel to each other (Fig. 1 and Table S3† show their directions for the ground KD on Yb1 and Yb2), which means that all exchange states are magnetic. The lack of axial symmetry in the Yb environments results in strong relative rotation of the main magnetic axes in the four KDs on each Yb site, like it was seen in other low-symmetry Ln complexes and fragments.[12] The obtained large transversal g factors on Yb ions (low magnetic axiality) and the relatively large tunnelling gap in the ground exchange doublet (*ca.* 0.01 cm^{-1}, Table S4†) are the reason for strong quantum tunnelling of magnetisation and for the lack of slow relaxation in **1** without an applied dc field.

In conclusion, we were able to synthesize a Yb_2 complex where slow magnetic relaxation was observed under an applied static dc field. Such field-induced SMM behaviour is due to low magnetic axiality and the large tunnelling gap leads to significant quantum tunnelling of the magnetisation. Complex **1** represents the first example of a polynuclear Yb^{III} SMM reported to date. This promising result allows us to envision and tailor new SMMs based on Yb^{III} ions and potentially create high-energy barrier SMMs.

Acknowledgements

This work was financially supported by the NSFC of China (21102039 and 21072049) and Heilongjiang Province (10td03), NSERC-DG, CFI, ORF and ERA Canada.

Notes and references

1 N. Ishikawa, M. Sugita, T. Ishikawa, S. Koshihara and Y. Kaizu, *J. Am. Chem. Soc.*, 2003, **125**, 8694.
2 (*a*) P.-H. Lin, T. J. Burchell, L. Ungur, L. F. Chibotaru, W. Wernsdorfer and M. Murugesu, *Angew. Chem., Int. Ed.*, 2009, **48**, 9489; (*b*) R. J. Blagg, C. A. Muryn, E. J. L. McInnes, F. Tuna and R. E. P. Winpenny, *Angew. Chem., Int. Ed.*, 2011, **50**, 6530; (*c*) J. D. Rinehart and J. R. Long, *Chem. Sci.*, 2011, **2**, 2078 and references therein; (*d*) F. Habib, P.-H. Lin, J. Long, I. Korobkov, W. Wernsdorfer and M. Murugesu, *J. Am. Chem. Soc.*, 2011, **133**, 8830.
3 (*a*) N. Lopez, A. V. Prosvirin, H. Zhao, W. Wernsdorfer and K. R. Dunbar, *Chem.–Eur. J.*, 2009, **15**, 11390; (*b*) J. D. Rinehart, M. Fang, W. J. Evans and J. R. Long, *J. Am. Chem. Soc.*, 2011, **133**, 14236; (*c*) N. Ishikawa, M. Sugita and W. Wernsdorfer, *Angew. Chem., Int. Ed.*, 2005, **44**, 2931.
4 (*a*) J. Long, F. Habib, P.-H. Lin, I. Korobkov, G. Enright, L. Ungur, W. Wernsdorfer, L. F. Chibotaru and M. Murugesu, *J. Am. Chem. Soc.*, 2011, **133**, 5319; (*b*) J. K. Tang, I. Hewitt, N. T. Madhu, G. Chastanet, W. Wernsdorfer, C. E. Anson, C. Benelli, R. Sessoli and A. K. Powell, *Angew. Chem.*, 2006, **118**, 1761; (*c*) C. E. Burrow, T. J. Burchell, P.-H. Lin, F. Habib, W. Wernsdorfer, R. Clérac and M. Murugesu, *Inorg. Chem.*, 2009, **48**, 8051.
5 R. J. Blagg, F. Tuna, E. J. L. McInnes and R. E. P. Winpenny, *Chem. Commun.*, 2011, **47**, 10587.
6 S.-D. Jiang, B.-W. Wang, H.-L. Sun, Z.-M. Wang and S. Gao, *J. Am. Chem. Soc.*, 2011, **133**, 4730.
7 (*a*) M. A. AlDamen, S. Cardona-Serra, J. M. Clemente-Juan, E. Coronado, A. Gaita-Arino, C. Marti-Gastaldo, F. Luis and O. Montero, *Inorg. Chem.*, 2009, **48**, 3467; (*b*) H. L. C. Feltham, F. Klower, S. A. Cameron, D. S. Larsen, Y. Lan, M. Tropiano, S. Faulkner, A. K. Powell and S. Brooker, *Dalton Trans.*, 2011, **40**, 11425; (*c*) M. Sugita, N. Ishikawa, T. Ishikawa, S. Koshihara and Y. Kaizu, *Inorg. Chem.*, 2006, **45**, 1299.
8 P.-H. Lin, W.-B. Sun, M.-F. Yu, G.-M. Li, P.-F. Yan and M. Murugesu, *Chem. Commun.*, 2011, **47**, 10993.
9 (*a*) T. D. Pasatoiu, C. Tiseanu, A. M. Madalan, B. Jurca, C. Duhayon, J. P. Sutter and M. Andruh, *Inorg. Chem.*, 2011, **50**, 5879; (*b*) P.-F. Yan, S. Chen, P. Chen, J.-W. Zhang and G.-M. Li, *Cryst. Eng. Commun.*, 2011, **13**, 36.

10 S. Zhao, X. Liu, W. Feng, X. Lu, W.-Y. Wong and W.-K. Wong, *Inorg. Chem. Commun.*, 2012, **20**, 41.
11 (*a*) F. Aquilante, L. De Vico, N. Ferré, G. Ghigo, P.-Å. Malmqvist, P. Neogrády, T. B. Pedersen, M. Pitonak, M. Reiher, B. O. Roos, L. Serrano-Andrés, M. Urban, V. Veryazov and R. Lindh, *J. Comput. Chem.*, 2010, **31**, 224; (*b*) For the description of the Single_Aniso module, see http://www.molcas.org/documentation/manual/node10.html
12 L. Ungur and L. F. Chibotaru, *Phys. Chem. Chem. Phys.*, 2011, **13**, 20086.

